doublet was initiated. This was done in part to confirm that the trim conditions were satisfied. But they are never exactly satisfied, and so after one second a small pitch rate is encountered. If the doublet was initiated at $t = 0$, the final altitude reduces to almost -2 ft, making the difference in the altitude histories even less.

These results show very good agreement between the linear and nonlinear simulations. However, if the elevator inputs were sufficiently large, such that the small-perturbation assumptions were no longer valid for the linear model, much larger differences would be observed between the two sets of results.

EXAMPLE 8.11

Case Study—A Nonlinear Aircraft-Performance Simulation[2]

In this case study we will develop a nonlinear performance simulation for a rigid aircraft operating in a steady wind (as opposed to gusts). This simulation will allow for the investigation of an aircraft's responses while following a desired flight profile. The profiles are defined in terms of commanded velocities, rates of climb, and/or headings, similar in some respects to commands given by air traffic control.

Up to this point in the chapter, we have always assumed that we wished to accurately simulate both the translational and rotational degrees of freedom of the vehicle. But now we wish to focus more on the translational performance of an aircraft being guided by a set of feedback guidance laws, and only approximate the attitude dynamics of the vehicle. This makes the simulation more numerically efficient, plus it allows us to avoid the details of an inner-loop attitude-control system at this stage of analysis. As we shall see, it also avoids the necessity of numerically solving for the initial trim flight condition.

We also take two other digressions here. The first is that the aircraft may be operating in a steady wind. If so, the air mass is assumed to be uniformly translating with respect to the earth-fixed inertial reference frame. The aerodynamic forces and moments acting on the vehicle depend on the vehicle's velocity (i.e., airspeed) and orientation relative to the air mass. And the presence of winds gives rise to differences between the vehicle's inertial velocity and its airspeed. Therefore, consistent with the material presented in Section 8.2.6, the presence of winds affects the forces on the vehicle. Finally, the simulation itself will be developed using the Simulink tools in MATLAB.

The equations of motion include a set of translational performance equations plus kinematic equations relating the vehicle's inertial position to its inertial velocity, all developed in Section 2.7. The translational equations of motion governing the magnitude and direction of the vehicle's inertial velocity (vector) were given in Equations (2.137), for a vehicle with propulsive thrust defined to be aligned with the fuselage-referenced X axis. Or

$$\begin{aligned} m\dot{V}_V &= T\cos\alpha\cos\beta - D - mg\sin\gamma \\ mV_V\left(\dot{\psi}_W\cos\phi_W\cos\gamma - \dot{\gamma}\sin\phi_W\right) &= \mathsf{S} + T\cos\alpha\sin\beta + mg\sin\phi_W\cos\gamma \\ mV_V\left(\dot{\gamma}\cos\phi_W + \dot{\psi}_W\sin\phi_W\cos\gamma\right) &= L + T\sin\alpha - mg\cos\phi_W\cos\gamma \end{aligned} \tag{8.157}$$

[2] This simulation is based on one developed by Dr. John Schierman while he served as a postdoctoral research associate in the Flight Dynamics and Control Lab, University of Maryland, College Park.

Note that γ, ϕ_W, and ψ_W are the flight-path angle, and wind-axes bank and heading angles, respectively, and that V_V is the inertial velocity of the vehicle.

We now assume that the vehicle's sideslip angle β and the aerodynamic side force S are both zero (as in steady, level flight or in a steady coordinated turn), and that the vehicle's angle of attack α is sufficiently small such that

$$T\cos\alpha \approx T, \quad T\sin\alpha \ll L \tag{8.158}$$

Under these assumptions, Equations (2.137) may be rearranged to become simply

$$\boxed{\begin{aligned} \dot{V}_V &= \frac{T-D}{m} - g\sin\gamma \\ \dot{\gamma} &= \frac{1}{mV_V}\left(L\cos\phi_W - mg\cos\gamma\right) \\ \dot{\psi}_W &= \frac{L\sin\phi_W}{mV_V\cos\gamma} \end{aligned}} \tag{8.159}$$

From Equations (8.159) we can readily see how the two forces thrust T and lift L (magnitude and direction) are used to control velocity, flight-path angle, and heading angle, respectively. The angle of attack is used to adjust the magnitude of the lift vector, while the wind-axes bank angle ϕ_W is used to rotate the orientation of the lift vector relative to the vehicle's velocity vector.

Let us now approximate the responses of the engine and airframe with the following transfer functions or first-order differential equations.

$$\boxed{\begin{aligned} \frac{T(s)}{T_c(s)} &= \frac{p_T}{s+p_T} & & \dot{T} = -p_T T + p_T T_c \\ \frac{L(s)}{L_c(s)} &= \frac{p_L}{s+p_L} & \text{or} \quad & \dot{L} = -p_L L + p_L L_c \\ \frac{\phi_W(s)}{\phi_{W_c}(s)} &= \frac{p_\phi}{s+p_\phi} & & \dot{\phi}_W = -p_\phi \phi_W + p_\phi \phi_c \end{aligned}} \tag{8.160}$$

The parameters p_T, p_L, and p_ϕ are time constants selected to approximate the responses of the engine and the airframe attitude. Also, let the limits on these responses be taken to be

$$0 \le T \le T_{\max}, \quad L \le K_{L_{\max}} V_V^2, \quad -\phi_{W_{\max}} \le \phi_W \le \phi_{W_{\max}} \tag{8.161}$$

where the maximum values again depend on the aircraft being simulated.

The three kinematic equations relating the vehicle's velocity to the inertial position were given in Equations (2.141), repeated here.

$$\boxed{\begin{aligned}\dot{X}_I &= V_V \cos\gamma \cos\psi_W \\ \dot{Y}_I &= V \cos\gamma \sin\psi_W \\ \dot{\mathrm{h}} &= V \sin\gamma\end{aligned}}$$

Finally, let the mass of the aircraft be given by the differential equation

$$\boxed{\dot{m} = -\dot{w}_f/g = -K_{\dot{w}} T} \tag{8.162}$$

with the initial condition $m = m_0$, where $\dot{w}_f$ is the fuel flow rate and $K_{\dot{w}}$ is a constant depending on the aircraft. So Equations (8.159–8.162), along with Equations (2.141) given above, constitute the equations of motion to be used in the simulation.

The model for the aerodynamic lift and drag is taken to be

$$\boxed{\begin{aligned}C_L &= C_{L_\alpha}(\alpha - \alpha_0) \\ C_D &= C_{D_0} + \frac{C_L^2}{K_D}\end{aligned}} \tag{8.163}$$

with

$$\boxed{L = C_L q_\infty S_W, \quad D = C_D q_\infty S_W, \quad q_\infty = \frac{1}{2}\rho_\infty V_\infty^2, \quad K_D = \pi A e_{\text{eff}}}$$

and note that in the presence of wind, $V_\infty \neq V_V$. The relation between these two velocities may be described as follows. Since the inertial velocity $\mathbf{V}_V$ is the vector sum of the velocity relative to the air mass $\mathbf{V}_\infty$ plus the wind velocity $\mathbf{W}$, or

$$\mathbf{V}_V = \mathbf{V}_\infty + \mathbf{W}$$

we have

$$\mathbf{V}_\infty = \mathbf{V}_V - \mathbf{W} \tag{8.164}$$

So then

$$\boxed{V_\infty = \sqrt{\dot{X}_W^2 + \dot{Y}_W^2 + \dot{\mathrm{h}}_W^2}} \tag{8.165}$$

where

$$\begin{aligned}\dot{X}_W &= V_V \cos\gamma \cos\psi_W - W_X \\ \dot{Y}_W &= V \cos\gamma \sin\psi_W - W_Y \\ \dot{\mathrm{h}}_W &= V \sin\gamma - W_h\end{aligned} \tag{8.166}$$

with the wind velocity vector given by

$$\mathbf{W} = W_X \mathbf{i}_I + W_Y \mathbf{j}_I - W_h \mathbf{k}_I \tag{8.167}$$

Now since we are using aerodynamic lift L directly as an independent or control variable in the equations of motion, we will "invert" Equations (8.163) to find the inferred angle of attack α and drag D for a given value of lift L. That is, we have

$$\begin{aligned} D &= K_{D_0} V_\infty^2 + K_{D_1} \frac{L^2}{V_\infty^2} \\ \alpha &= K_L \frac{L}{V_\infty^2} + \alpha_0 \end{aligned} \tag{8.168}$$

with

$$K_{D_0} = \frac{1}{2}\rho_\infty S_W C_{D_0}, \quad K_{D_1} = \frac{2}{\rho_\infty S_W K_D}, \quad K_L = \frac{2}{\rho_\infty S_W C_{L_\alpha}}$$

Of course, all these aerodynamic parameters also depend on the vehicle. This completes the mathematical model of the vehicle's dynamics.

The guidance laws given in Equations (8.169) provide the commanded thrust T_c, lift L_c, and bank angle ϕ_{Wc} by feeding back the relevant inertial-velocity, inertial-velocity-heading, and inertial rate-of-climb and comparing them to commanded values. The commanded velocity V_c, rate of climb $\dot{h}_c = V_c \sin\gamma_c$, and heading ψ_c are user-defined inputs to the simulation that describe the desired trajectory. The mathematic model is now complete.

$$\frac{T_c(s)}{V_E(s)} = \frac{mK_{T_P}\left(s + \left(K_{T_I}/K_{T_P}\right)\right)}{s} \qquad \dot{x}_T = mV_E$$

$$T_c = K_{T_I} x_T + K_{T_P} m V_E, \quad V_E \triangleq \left(V_c - V_V\right)$$

$$\frac{L_c(s)}{\dot{h}_E(s)} = \frac{mK_{L_P}\left(s + \left(K_{L_I}/K_{L_P}\right)\right)}{s} \quad \text{or} \quad \dot{x}_L = m\dot{h}_E$$

$$L_c = K_{L_I} x_L + K_{L_P} m\dot{h}_E, \quad \dot{h}_E \triangleq V_c\left(\sin\gamma_c - \sin\gamma\right)$$

$$\frac{\phi_{W_c}}{\psi_E} = K_{\phi_P}\left(V_c/g\right) \qquad \phi_{W_c} = K_{\phi_P}\left(V_c/g\right)\psi_E, \quad \psi_E \triangleq \left(\psi_c - \psi_W\right)$$

(8.169)

In the case to be investigated, let the vehicle to be simulated be a large turbo-prop transport aircraft, similar to the C-130 aircraft shown in Figure 8.23. The modeling data for the aircraft is given in Table 8.4, while the values of the gains in the guidance laws for this vehicle are given in Table 8.5.

We are now ready to perform the simulation. Let the initial conditions be as follows:

$V_0 = 400$ mph (347 kts) (inertial velocity)

$\gamma_0 = 0$ (flight-path angle)

$\psi_{W_0} = 0$ (velocity-heading angle = north)

Figure 8.23 C-130 Aircraft. (Photo courtesy of NASA)

Table 8.4 Time Constants and Other Vehicle-Dependent Parameters

Weight, mg = 157,000–327,000 lbs		Airspeed Range, 200–600 mph	
$p_T = 2$ rad/sec	$T_{\max} = 72{,}000$ lbs	$K_{\dot{w}} = 4 \times 10^{-6}$ sl/(lbs-sec)	$\alpha_0 = -0.05$ deg
$p_L = 2.5$ rad/sec	$K_{L\max} = 2.6$ lbs/fps^2	$K_{D_1} = 2.48 \times 10^{-2}$ ft^2/lb-sec^2	$K_L = 5.24$ deg-ft/sl
$p_\phi = 1$ rad/sec	$\phi_{W_{\max}} = 30$ deg	$K_{D_0} = 3.8 \times 10^{-2}$ sl/ft	

Table 8.5 Gains in the Guidance Laws

$K_{T_P} = 0.08$ sec	$K_{T_I} = 0.002$/sec^2	$K_{L_P} = 0.5$/sec	$K_{L_I} = 0.01$/sec^2	$K_{\phi_P} = 0.075$ sec

And let the commanded inertial velocity, flight-path angle (or rate of climb), and velocity heading be

$$V_c = 450 \text{ mph } (391 \text{ kts}), \quad \gamma_c = 5 \text{ deg } (\dot{h}_c = 3455 \text{ fpm}), \quad \psi_c = 15 \text{ deg}$$

So the vehicle must transition from level flight in a northerly direction at 400 mph to a heading of 15 deg at 450 mph while climbing at approximately 3500 fpm. A steady wind of about 30 mph from the southwest ($W_X = W_Y = 25$ mph, $W_h = 0$) is included. And we wish to simulate the vehicle's dynamics for two minutes and evaluate its responses.

As noted earlier, this simulation was performed using the MATLAB tool Simulink. The block diagram used in the Simulink simulation is shown in Figure 8.24. Initially, the various simulation parameters are set using a MATLAB script or m file named perfsim.m (included in the accompanying set of MATLAB files located at www.mhhe.com/schmidt).

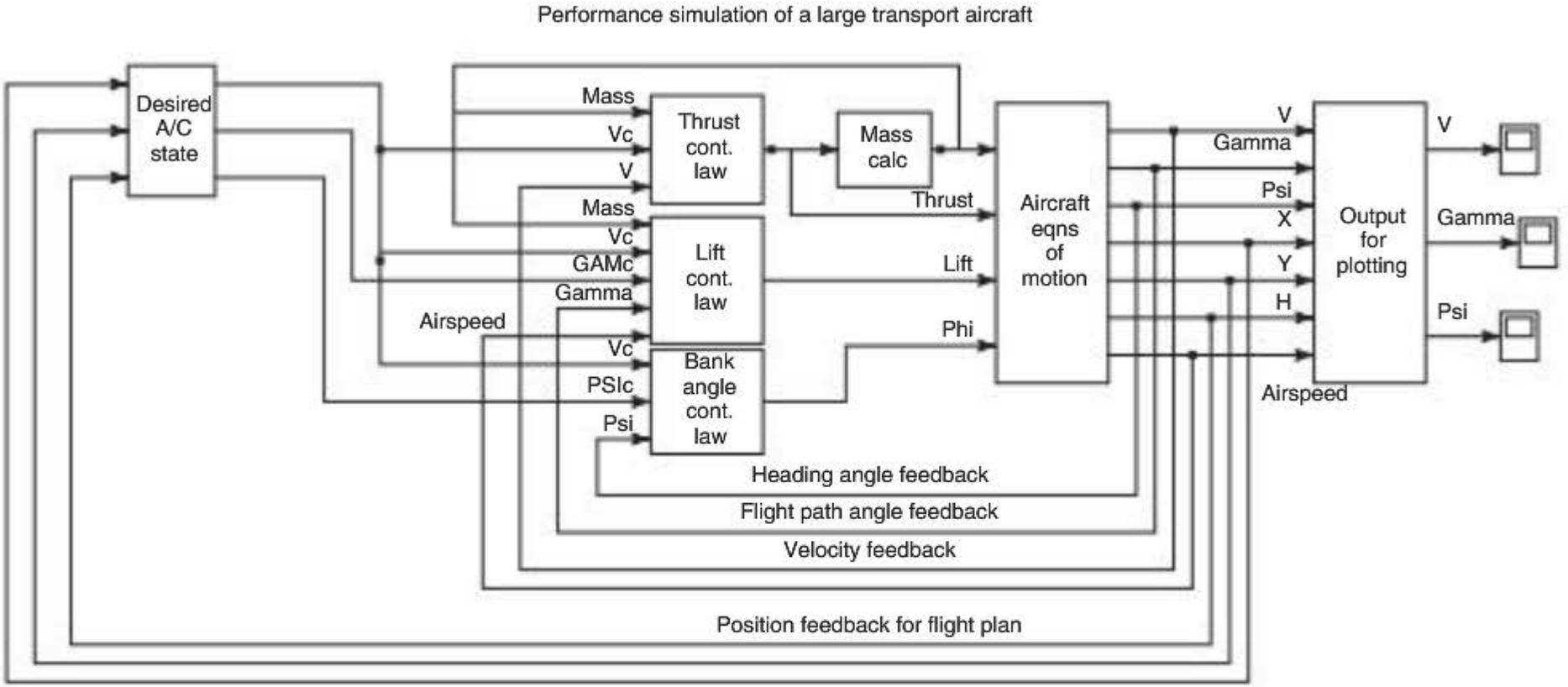

Figure 8.24 Simulink simulation diagram.

Then the Simulink model is executed for the desired simulated time of two minutes. And finally, another script file called plothist.m (also included in the accompanying set of MATLAB files) is used to plot the desired responses. The following results reveal that the vehicle responses indeed follow the desired trajectory.

The time histories of the airspeed V_∞, inertial velocity V_V, and thrust are shown first in Figure 8.25. The commanded inertial velocity is reached in approximately one minute. Since a significant increase in both airspeed and flight-path angle is commanded, a large increase in thrust is required. But this thrust does not exceed the maximum available thrust set in the model.

Next shown in Figure 8.26 are the time histories of the inertial flight-path angle and the inertial rate of climb, both compared to their commanded values, while in Figure 8.27

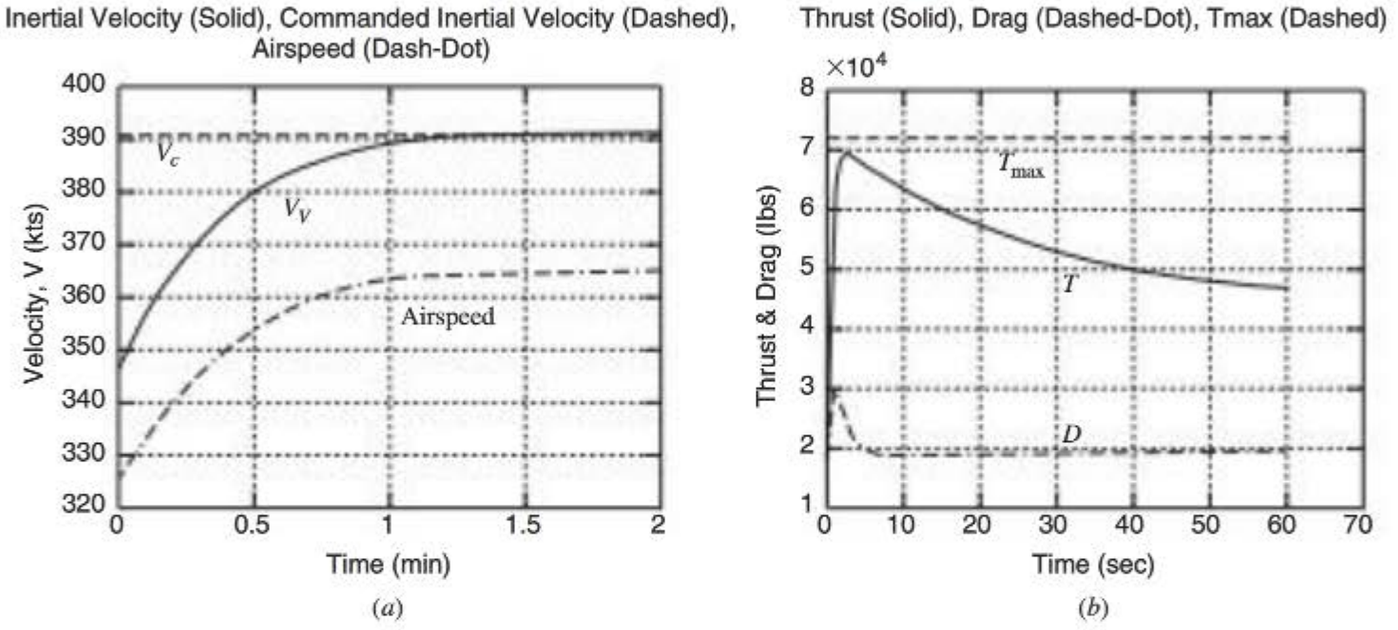

Figure 8.25 Time histories of velocities, thrust, and drag.

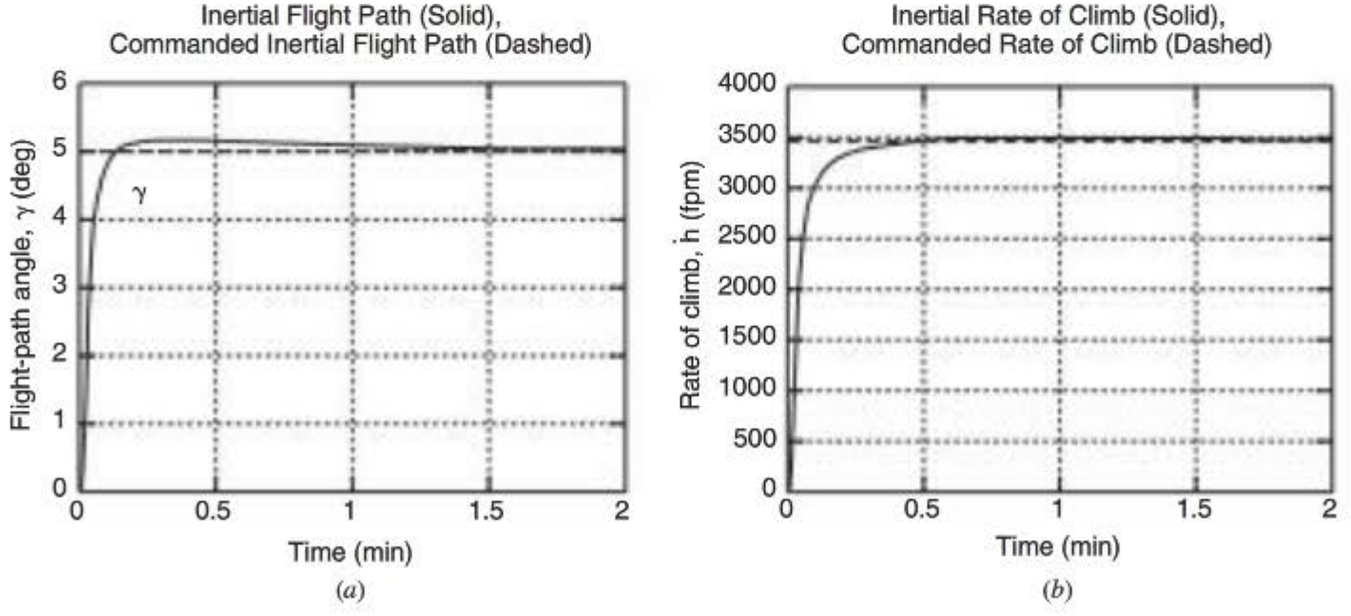

Figure 8.26 Time histories of flight-path angles and rates of climb.

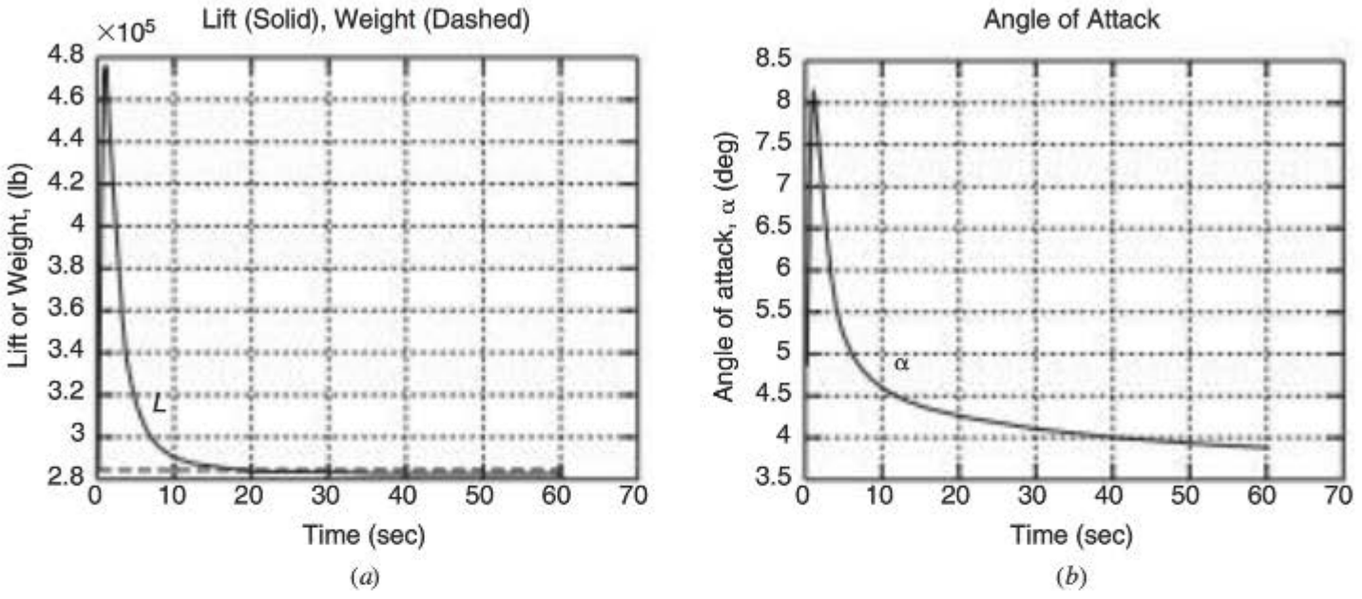

Figure 8.27 Time histories of lift, weight, and angle of attack.

the corresponding lift, weight, and angle-of-attack time histories are shown. The change in flight-path angle is rather rapid, reaching the commanded value in approximately 5 seconds. As shown in Figure 8.27*a*, a fairly aggressive increase in lift is required (due to the desired change in flight path as well as heading), which results in a peak vertical acceleration of approximately 1.7 g's. The maximum angle of attack of 8 deg, shown in Figure 8.27*b*, is achieved at approximately 1.5 seconds.

And finally we have the time history of the inertial heading compared to the commanded value, along with the corresponding bank-angle history, all shown in Figure 8.28. Note that the desired change in heading is accomplished smoothly in less than one minute. The maximum bank angle of slightly over 18 degrees occurs at about 3 sec.

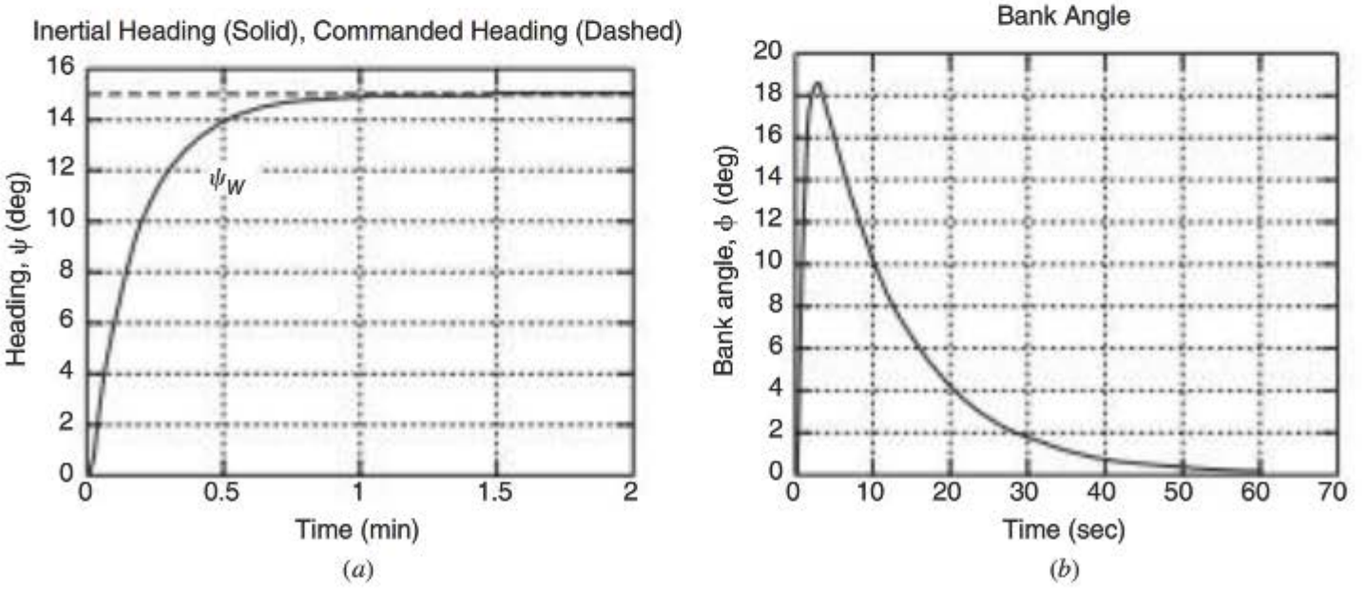

Figure 8.28 Time histories of inertial heading and bank angle.